

2
3 **In situ granulation by thermal stress during subaqueous volcanic eruptions**

4
5 Mathieu Colombier¹, Bettina Scheu¹, Ulrich Kueppers¹, Shane J. Cronin², Sebastian B. Mueller³,
6 Fabian B. Wadsworth¹, Manuela Tost², Kai-Uwe Hess¹, Katherine J. Dobson⁴,
7 Bernhard Ruthensteiner⁵, Donald B. Dingwell¹

8 ¹Department of Earth and Environmental Sciences, Ludwig-Maximilians-Universität München,
9 Germany, ²School of Environment, University of Auckland, New Zealand, ³Geology and Geophysics,
10 University of Hawai'i at Mānoa, Honolulu, Hawaii, USA, ⁴Department of Earth Sciences, Durham
11 University, UK, ⁵Bavarian State Collection of Zoology, Germany. *e-mail:

12 mathieu.colombier@min.uni-muenchen.de

13
14
15 This data repository contains:

- 16 (1) A description of the geological setting.
17 (2) A description of the scan conditions during the XCT analysis (including Table DR1).
18 (3) A brief discussion on the effect of crystals on crack propagation (including Figure DR1).

1) Geological setting: The Surtseyan eruptions of Capelinhos (1957-1958) and Hunga

Tonga-Hunga Ha'apai (2014-2015)

Capelinhos: The eruption off the western tip of Faial island (Azores, Portugal) lasted from September 1957 through October 1958. Eruptions were sporadic and included at least two cycles of shift from phreatomagmatic to magmatic as water became progressively excluded from the vent (Machado et al., 1962). The newly formed island joined onto Faial with much of the tephra also dispersed onto the existing island (Cole et al., 2001). The samples here were from primary fall deposits at the western and northern beach. The units comprised loose, cm- to dm-thick beds of mainly massive or weakly stratified, poorly sorted ash-lapilli tuffs (~2-4 mm modal particle size).

Hunga Tonga-Hunga Ha'apai: The eruption occurred in the intra-oceanic Tonga-Kermadec arc ~67 km north-northwest of Nuku'alofa (Kingdom of Tonga) between two existing islands of Hunga Tonga and Hunga Ha'apai. The activity lasted between 19th of September 2014 and 24th of January 2015 and formed a new near-circular tephra cone, ~120 m high and 2 km wide that coalesced with the pre-existing islands. The edifice was constructed by alternating tephra jets (up to 750 m high) and base surges, accompanied by fall from steam and ash plumes that rose up to 10 km into the atmosphere. Cancellation of international flights on the 13th and 14th of January were caused by ash dispersed up to 870 km from the volcano (Global Volcanism Program, 2015). The samples analysed here were collected from fall deposits from the margins of the new cone and base surge deposits extending onto the pre-existing islands (~3-5 mm modal particle size).

2) XCT analysis

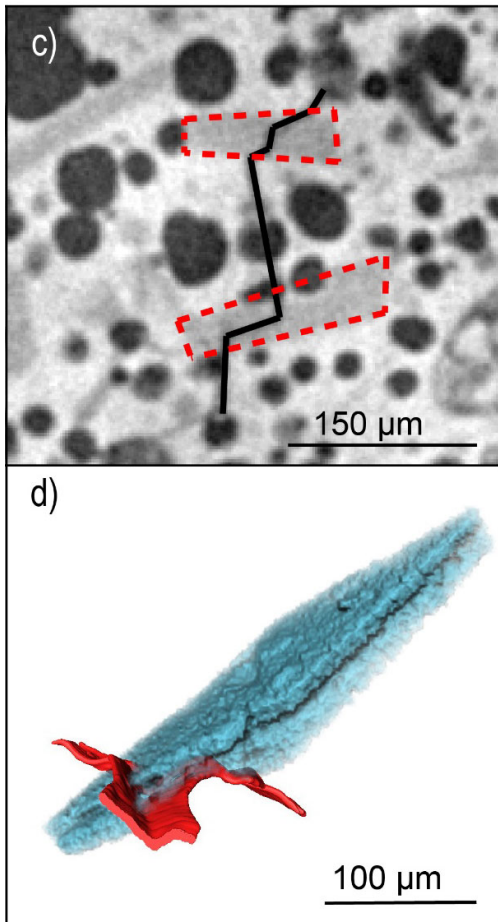
Scanning was performed using a GE[®] Phoenix Nanotom laboratory scanner (Obermenzing, Germany). We used an aluminum filter with a thickness of 0.1-0.2 mm, a current ranging from 135 to 170 nA and a voltage of 90 to 100 kV and achieved voxel sizes of between 1.55 and 2.40 μm . Specific scan conditions for each sample are given in Table 1 in the Supplementary material. Reconstruction was performed using GE[®] proprietary software and image processing was carried out using Avizo[®] (FEI). We additionally analysed 6 ash-encased lapilli from Hunga Tonga-Hunga Ha'apai using back-scattered electron images (SU 5000 Schottky FE-SEM, HITACHI). SEM observations are consistent

61 with the XCT analysis.

62 3) Role of crystals on crack propagation

63 Cracks commonly change their propagation direction at crystal-glass boundaries. This influences the
64 morphology of the ash grains produced by in situ granulation.

65



66

67 **Figure DR1.** Role of crystals on crack propagation. (A) 2D and (B) 3D XCT images cracks changing
68 their direction of propagation when intersecting crystals in sample CAP370-3-1 (blue). The crack in
69 (A) appears in black and crystals in dashed red line. The crack in (B) appears in red and the crystal in
70 blue.

Samle name	Deposit type	Filter	Voltage (kV)	Current (nA)	Timing (s)	Nb images	Vesicularity	Connectivity
HH28-1	Fall	0.2 Al	100	135	2000	1000	-	-
HH28-3	Fall	0.2 Al	90	170	1000	1440	0.26 ^a	0.33 ^a
HH47-1	Surge	0.1 Al	90	170	1000	1201	0.54 ^a	1.00 ^a
HH47-2	Surge	0.2 Al	90	170	1000	1440	0.64 ^a	0.99 ^a
CAP370-3-1	Lithofacies III/IV in Cole et al., (2001)	0.1 Al	80	180	1250	1440	0.28	0.5
CAP-370-2		0.1 Al	80	180	1250	1440	0.39	0.87
CAP-372-3		0.1 Al	80	180	1250	1440	0.46	0.97

71

72 **Table DR1.** Sample name, deposit type and scan conditions for the ash-encased lapilli analysed by

73 XCT. The vesicularity and vesicle connectivity of the cores of the ash-encased lapilli are included.

74 The superscript ^a refers to values taken from Colombier et al. (2018).